JACS
JOURNAL OF THE AMERICAN CHEMICAL SOCIETY
pubs.acs.org/JACS
Article

# Regulating Chemically Fueled Peptide Assemblies by Molecular Design

Kun Dai, Jennifer Rodon Fores, Caren Wanzke, Benjamin Winkeljann, Alexander M. Bergmann, Oliver Lieleg, and Job Boekhoven*

Cite This: J. Am. Chem. Soc. 2020, 142, 14142−14149
Read Online
ACCESS | Metrics & More | Article Recommendations | Supporting Information

**ABSTRACT:** In living systems, fuel-driven assembly is ubiquitous, and examples include the formation of microtubules or actin bundles. These structures have inspired researchers to develop synthetic counterparts, leading to exciting new behaviors in man-made structures. However, most of these examples are serendipitous discoveries because clear design rules do not yet exist. In this work, we show design rules to drive peptide self-assembly regulated by a fuel-driven reaction cycle. We demonstrate that, by altering the ratio of attractive to repulsive interactions between peptides, the behavior can be toggled between no assembly, fuel-driven dissipative self-assembly, and a state in which the system is permanently assembled. These rules can be generalized for other peptide sequences. In addition, our finding is explained in the context of the energy landscapes of self-assembly. We anticipate that our design rules can further aid the field and help the development of autonomous materials with life-like properties.

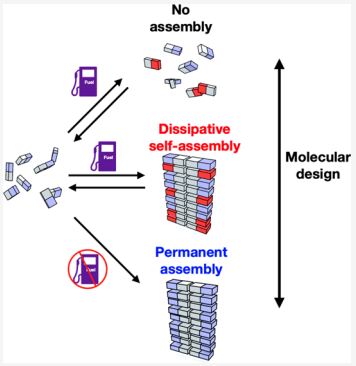


Downloaded via TU MUENCHEN on September 15, 2020 at 12:46:05 (UTC).
See https://pubs.acs.org/sharingguidelines for options on how to legitimately share published articles.

## INTRODUCTION

The construction of dissipative self-assembling systems aims at the construction of assemblies that possess the dynamic behavior we observe in living systems.[1−6] Inspired by the self-assembly of microtubules fueled by the hydrolysis of GTP,[7] or the formation of actin bundles by the conversion of ATP,[8] researchers have developed chemical reaction cycles that can be used to drive dissipative assembly of small molecules or nanoparticles.[9,10] In these chemical reaction cycles, an activation reaction converts a precursor molecule into a self-assembling product driven by the irreversible conversion of a high-energy reagent. A deactivation reaction reverts the product to the original precursor spontaneously. Thus, the chemical energy that is obtained by the conversion of the high energy reagent into waste is temporarily stored in a transient modification of the precursor molecule.[5,11,12] We, and others, refer to the high-energy molecule as a chemical fuel. That chemical change can be used to induce self-assembly. However, due to the transient nature of the product, it will disassemble upon reversion to the precursor. As a consequence of the dynamic interplay between product activation and deactivation, the assembly and disassembly are dynamic too, which results in emerging structures that possess behavior that we typically do not observe in equilibrium. Examples of dissipative assembly include the formation of fibers driven by the hydrolysis of methylation agents,[13] the formation of supramolecular polymers by the reduction of oxidizing agents[14,15] or by the hydrolysis of ATP,[16] the formation of active droplets at the expense of a condensing agent,[17,18] and others.[19−27] Exciting behaviors observed in these assemblies contain the dynamic instabilities found in synthetic self-assembled fibers[28] and solutions spontaneously oscillated from one self-assembled state to another driven by a chemical fuel.[15]

Despite the recent progress in the field, it remains challenging to design molecules in order to ensure that the energy harvested by the chemical reaction cycle is optimally used to induce dynamic assembly. Thus, in this work, we introduce two approaches to control the fuel-driven self-assembly of peptides by molecular design. In one approach, the amount of attractive interactions between peptides is tuned, allowing to toggle the fuel-driven behavior from no assembly, chemically fueled dissipative self-assembly to static self-assembly. In another approach, the repulsive interactions between peptides are tuned, resulting in similar control. We rationalize our findings with the energy landscapes associated with the self-assembly and chemical reaction cycle.

## RESULTS AND DISCUSSION

**Description of the Chemical Reaction Cycle.** In this work, we use a chemical reaction cycle that transiently activates a building block for self-assembly (Figure 1A).[18,29−31] In the cycle, a molecular precursor reacts with a high-energy molecule

Received: April 17, 2020
Published: July 27, 2020




© 2020 American Chemical Society

https://dx.doi.org/10.1021/jacs.0c04203
J. Am. Chem. Soc. 2020, 142, 14142−14149

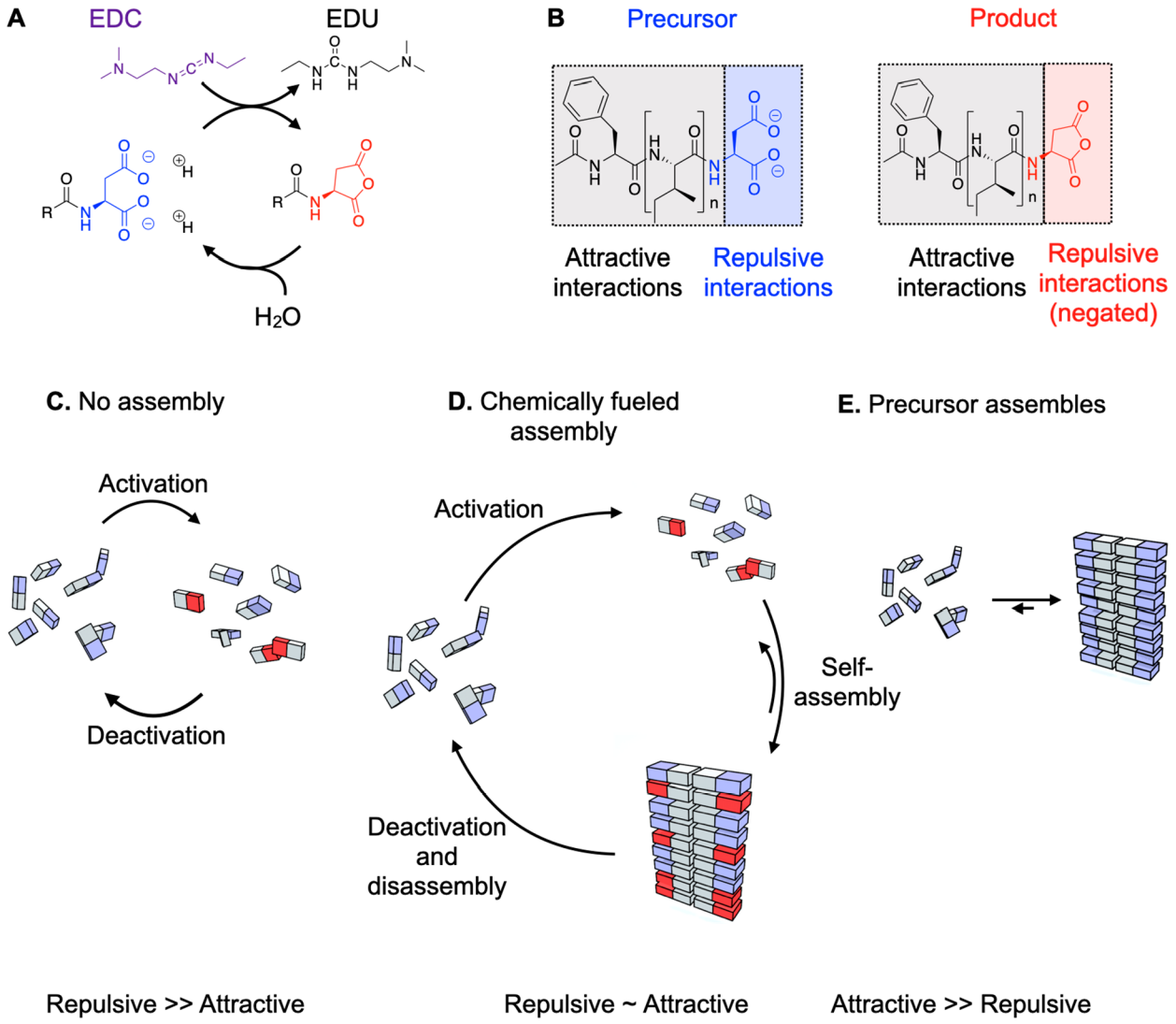


**Figure 1.** Design strategy for dissipative self-assembly. (A) A chemical reaction cycle is used that comprises an activation and deactivation reaction. In the activation reaction, aspartic acid derivatives react with carbodiimide EDC and are converted to their corresponding anhydride. In the deactivation reaction the aspartic acid anhydride derivative is hydrolyzed. When correctly designed, the transient aspartic acid anhydride can self-assemble, but the aspartic acid derivative cannot. (B) Molecular structure of the precursors and products used in this work. (C–E) The balance between attractive and repulsive interactions can affect the fuel-driven response of the reaction cycle. When the attractive interactions are much weaker than the repulsive interactions, no assembly is formed (C). When the attractive interactions are balanced with the repulsive interactions, dissipative assemblies can form (D). When the attractive interactions are too strong, the precursor can self-assemble without fuel (E).

(fuel) to form a product. That reaction is referred to as the activation reaction. The activation is irreversible; that is, the fuel is irreversibly "burned". A second reaction spontaneously deactivates the product and yields the precursor. Consequently, the product is metastable with a half-life determined by the deactivation rate.

We used a chemical reaction cycle to regulate the assembly and disassembly of peptides building blocks. In the cycle, aspartic acid derivatives are converted into their corresponding anhydride state by the consumption of a condensing agent, ethyl-3-(3-(dimethylamino)propyl) carbodiimide (EDC). This reaction constitutes the activation reaction. Simultaneously, the anhydride is hydrolyzed. This constitutes the deactivation reaction. When the peptide is correctly designed, its transient anhydride can self-assemble, but the aspartic acid derivative cannot. In effect, the assembly and disassembly of the derivatives is regulated by the formation and hydrolysis of aspartic acid anhydride. We introduced this cycle in previous work.[18,25,26,29−32] As a precursor, we used peptides that carry a C-terminal aspartic acid (D). These peptides thus carry two dicarboxylate groups, which are converted into their corresponding cyclic anhydride at the expense of a molecule of carbodiimide (Figure 1A). However, in the aqueous environment, the anhydride product is hydrolyzed back to the precursor, which constitutes the spontaneous deactivation reaction.

**Design of the Precursors.** Our design strategy for the precursor is to use the loss of negative charges on the carboxylate precursor to induce the self-assembly of the product (Figure 1B). The carboxylates of the precursor have a $pK_A$ in the range of 1.9 and 3.9. Under the employed conditions, the precursors are expected to have an ionic charge of −2 (pH 6, 15 mM precursor, 200 mM 2-(*N*-morpholino)-ethanesulfonic acid (MES) buffer). Moreover, we found in earlier work that, at this pH, the balance of the pH-dependent activation and deactivation is sufficient to ensure the formation


https://dx.doi.org/10.1021/jacs.0c04203
J. Am. Chem. Soc. 2020, 142, 14142−14149

of significant amounts of product.[29] In contrast, upon EDC-induced activation, the two carboxylates condense into a charge-neutral anhydride product. Typically, the loss of the two anions is used to regulate the self-assembly behavior of the system to fuel. We categorize the self-assembly behavior in three classes, i.e., fuel is added, and no self-assembly is observed (no assembly, Figure 1C). Fuel is added, and transient assembly is observed (dissipative self-assembly, Figure 1D). The precursor assembles without the addition of fuel (precursor assembles, Figure 1E). While our interest is in chemically fueled dissipative self-assembly, we frequently encounter the other two scenarios (no assembly or precursor assemblies).

The aim of the first part of this study is to understand how attractive interactions can be used to regulate the response of the system to chemical fuel. We tuned the degree of attractive interactions between the molecules in the chemical reaction cycle by varying the peptide segment (Figure 2A). We

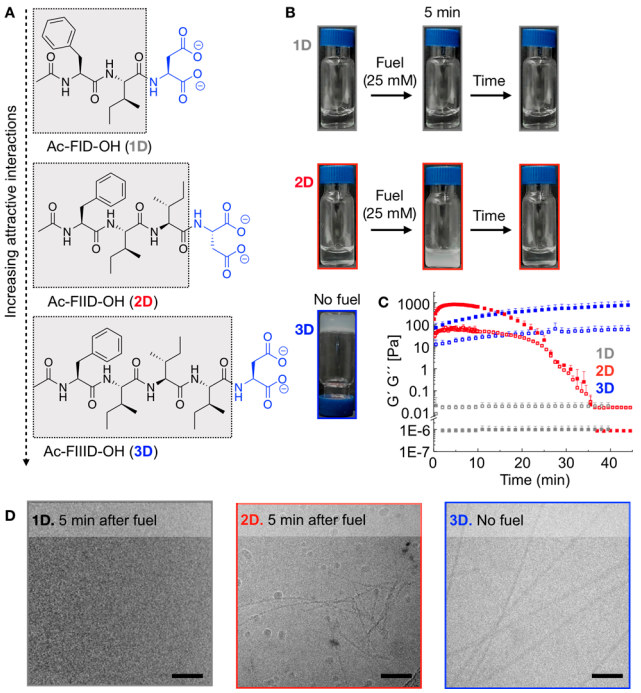


**Figure 2.** Regulating the response to fuel by tuning the attractive interactions. (A) Molecular structures of peptide **1D**, **2D**, and **3D** used as precursors. (B–D) Assessment of the self-assembly behavior of **1D** or **2D** before and after the addition of 25 mM fuel and **3D** without fuel. (B) Photographs of the solutions. (C) Storage and loss modulus as a function of time. The solid squares represent the storage modulus (G′); open squares represent the loss modulus (G″). Error bars represent the standard deviation of the mean ($n$ = 3). (D) Cryo-TEM micrographs. All scale bars correspond to 100 nm. All the experiments were carried out at a peptide concentration of 15 mM, a pH of 6, and in 200 mM MES buffer.

synthesized the precursors Ac-FID-OH (**1D**), Ac-FIID-OH (**2D**), and Ac-FIIID-OH (**3D**), where F stands for phenylalanine, I for isoleucine, and D for aspartic acid. The rationale behind the molecular design is as follows: the aspartic acid is the chemically active unit that switches its degree of electrostatic repulsion by the chemical reaction cycle. In line with recent work by Webber and co-workers,[33] the F and I amino acids were introduced in order to promote fiber formation via $\pi$-orbital overlap, hydrogen bond formation, and hydrophobic interactions. The number of I (1–3) allowed us to test the response of the system with an increasing degree of attractive interactions. Finally, it is worth mentioning that the phenyl group of the F greatly facilitates the characterization of the products of the chemical reaction cycle by HPLC due to its aromatic group. We tested the behavior of the precursors with a thioflavin-T (ThT) assay before the addition of fuel. ThT is a fluorescent dye that drastically increases its fluorescence intensity when bound to structured assemblies like fibers. We found no evidence for fiber formation for **1D** and **2D**. In contrast, **3D** did show an increased intensity, which is evidence of fiber formation before the addition of EDC as fuel (Figure S1).

By analytical HPLC, the evolution of the reaction cycle of precursors **1D** and **2D** was tested after the application of 25 mM EDC as fuel. Both precursors consumed the 25 mM EDC within 40 min, and the consumption could be fitted with a second-order rate constant (Table S2). The corresponding anhydride was observed within the first minute and peaked between 5 and 10 min before it collapsed until no more anhydride was observed after 40 min (Figures S2, S3, S4). Using a previously described kinetic model,[30] we could fit the evolution of relevant reactants in the cycle. That means that we can predict the concentration of each species for every second after the application of fuel. We describe the model in more detail in the Supporting Note 1.

We studied how the emergence and decay of the anhydride affected the macroscopic properties of peptide **1D**. We added 25 mM EDC to peptide **1D**; however, in all cases, the solution remained optically transparent (Figure 2B). To further verify the lack of assembly in response to fuel, we quantified the turbidity by measuring the absorbance at 600 nm as a function of time in response to 25 and 400 mM EDC (Figure S5B). Neither amount of fuel resulted in increased turbidity. Similarly, a ThT assay did not show an increased signal in response to a large amount of fuel (Figure S6). Rheology measurements showed that 15 mM **1D** behaved like a liquid ($G'' \gg G'$) even after the addition of 25 mM EDC (Figure 2C). One can observe a high signal of $G''$ for the first point, which is an artifact caused by the inertia of the measuring system. Finally, cryo-TEM showed no obvious assemblies present in the sample after fueling (25 mM EDC, Figure 2D). Taken together, the data show that peptide **1D** does not assemble in response to fuel.

In contrast, 25 mM EDC added to peptide **2D** resulted in the rapid formation of a weak turbid hydrogel; that is, within 1 min, the solution turned turbid and viscous (Figure 2B). After around 40 min, the solution regained its original viscosity and transparency. We carried out turbidity measurements by monitoring the absorbance at 600 nm, which could quantify the increased turbidity in response to 25 mM EDC (Figure S5C). It is worth mentioning that when we used up to 400 mM EDC, **2D** still underwent transient self-assembly (Figure S5C). Moreover, we found that the duration of the turbidity increased with increasing amounts of EDC (Figure S5C). A ThT assay showed a drastic increase in signal in response to EDC, indicative of beta-sheet formation between the peptides (Figure S6). By means of rheology, we found that 15 mM **2D** behaved like a liquid ($G'' \gg G'$) before the addition of 25 mM EDC (Figure S5D), but rapidly converted into an elastic hydrogel after the addition of fuel ($G' > G''$). As the gel formation is very fast, no sol–gel transition is observed upon fuel addition. The increased viscosity was transient, and the


https://dx.doi.org/10.1021/jacs.0c04203
J. Am. Chem. Soc. 2020, 142, 14142–14149

sample was kept in a semistable state before collapsing after 35 min. A cryo-TEM study showed no obvious assemblies before the addition of EDC (Figure S7). However, 5 min after the addition of fuel, we found relatively short fibers (Figure 2D).

To better understand the dissipative self-assembly of peptide **2D**, we measured the fiber composition by a $^1$H NMR study.[30] We used the fact that self-assembled peptides have a reduced transversal relaxation time (T2), resulting in long correlation times and a broadening of the signal that gets hidden under the baseline. This means that peptides, which participate in the assembly, become NMR-silent, while soluble peptides were NMR-visible. Seven minutes after the addition of 25 mM fuel, we found that roughly 5 mM of the peptide remained in solution. In other words, 10 mM of peptide had assembled into fibers. We used the kinetic model to calculate the amount of product at this point in time and were surprised to observe that only 3 mM of the peptide was in the product state. In other words, if we assume all product was in the fibers, the fibers comprised roughly 70% of precursor, indicating a great amount of coassembly of precursor and product (Figure S8). Taken together, the combined data clearly show that peptide **2D** transiently assembles into fibers at the expense of EDC. These fibers comprise both the precursor and the anhydride product.

Finally, we found that peptide **3D** was able to assemble into an elastic hydrogel without the addition of EDC (Figurs 2B and C, S5A, S6). Moreover, cryo-TEM revealed that the peptide self-assembled into long fibers (Figure 2D). From these observations, we can conclude that the degree of attractive interactions between peptides can regulate the nonequilibrium response of the molecules to a chemical fuel. Peptide **1D**, with a relatively low degree of attractive interactions, underwent no assembly in response to fuel (Figure 1; no assembly). Peptide **2D** could undergo dissipative self-assembly (Figure 1; dissipative self-assembly). Finally, for the assembly of peptide **3D**, no fuel was required (Figure 1; precursor assembles).

Taken together, the data above show that the molecular design of our peptide can affect the response of the system to chemical fuel. We can draw out the following design rules that apply when the energy-dissipating chemical reaction cycle modulates the electrostatic repulsion between peptides. (i) If the attractive interactions are weak, the precursor will not assemble, and the product will not be able to assemble or coassemble with the precursor; that is, no assembly will occur upon fueling the system. (ii) If the attractive interactions are optimized, the peptide will not assemble in the precursor state but in the product state, leading to a coassembly with the precursor. (iii) Moreover, the coassembly will collapse when reverted to the precursor; that is, dissipative self-assembly will occur upon fueling the system. (iv) Finally, when the attractive interactions are too strong, the peptide will assemble in its precursor state; that is, no fuel is required to assemble the system.

In order to generalize our rules, we synthesized Ac-FV$_n$D-OH, where $n$ = 1, 2, 3, or 4. We measured the response of these peptides to fuel by turbidity measurements (Figure S9). In line with the data above, the peptides with weak attractive interactions (Ac-FVD-OH and Ac-FVVD-OH) did not show any increased turbidity in response to 25 mM EDC (i.e., no assembly). The turbidity of the solution of Ac-FVVVD-OH did increase, and the solution also became more viscous. Moreover, the increased turbidity and the formation of an elastic hydrogel was transient (i.e., dissipative self-assembly). Finally, Ac-FVVVVD-OH, like **3D**, formed a turbid hydrogel prior to the addition of EDC (i.e., the precursor assembled).

Regulating the response of our peptide to fuel by altering the degree of attractive interactions prompted us to study the opposite effect; that is, can we control the peptide's behavior by tuning repulsive interactions? The precursor in our reaction scheme is designed such that it does not assemble because it carries two negative charges that overcome the attractive interactions. We also observed that large amounts of precursor coassemble with the uncharged products. In other words, in the cases where we did not observe fuel-induced self-assembly, the attractive interactions were not sufficiently strong to overcome the electrostatic repulsion between the coassembling precursors. Thus, we reasoned that the addition of salts decreases the Debye screening length and results in a decrease of the electrostatic repulsion between precursors (Figure 3A).[34] Namely, additional salt could transition the response of peptides from dissipative self-assembly to a state where the precursor assembles. Moreover, given the fact that precursor and product coassemble to a large degree, the addition of salts could force nonassembling peptides to undergo fuel-driven dissipative self-assembly.

As demonstrated above, peptide **1D** did not assemble in response to EDC as fuel when dissolved in 200 mM MES buffer. In contrast, when peptide **1D** was dissolved in 200 mM MES buffer with 5 M NaCl, it transiently increased the turbidity in response to 25 mM EDC (Figure 3B), which we could quantify by measuring the absorbance at 600 nm (Figure 3C). A ThT assay demonstrated that peptide **1D** with 5 M NaCl did not engage in beta-sheet formation before fuel addition, but did transiently form beta-sheets in response to fuel (Figure S10A,B). The rheology measurements showed only a small increase in the viscoelastic properties upon addition of fuel, but no formation of an elastic hydrogel (Figure S10C). Cryo-TEM revealed that the peptide self-assembled into fibers after the addition of salt in response to the same concentration of fuel (Figure 3E). The above experiments show that the addition of a large amount of salt can change the behavior from a nonassembling peptide to a dissipative assembling peptide.

We showed that without additional salts, peptide **2D** could undergo fuel-driven dissipative self-assembly. In contrast, when we added 3 M or more NaCl, the peptide assembled into an elastic hydrogel without the addition of EDC (Figure 3B). We quantified the turbidity by measuring the absorbance at 600 nm (Figure S11A), and we measured the gel stiffness by rheology measurements (Figure 3D). A ThT assay indicated that the hydrogel formation was partially driven by beta-sheet formation (Figure S11B). Moreover, cryo-TEM revealed the presence of fibers without any fuel addition (Figure 3E). We were interested whether the self-assembly behavior of **2D** could be modulated by the pH of the solution. We decreased the pH from 6 to 4 by addition of HCl, and the clear solution turned turbid (Figure S12A). The static nature of the assemblies allowed performing a cryo-TEM study (Figure S12B). In contrast, if we increased the pH to 7, we found no more evidence of self-assembly, also in response to 25 mM of fuel. The lack of assemblies is likely a combination of increased charge−charge repulsion between the precursors and a lower maximum anhydride concentration, as the optimal pH of the reaction cycle is pH 6. These combined experiments show that a peptide that transiently assembled driven by a chemical fuel


https://dx.doi.org/10.1021/jacs.0c04203
J. Am. Chem. Soc. 2020, 142, 14142−14149

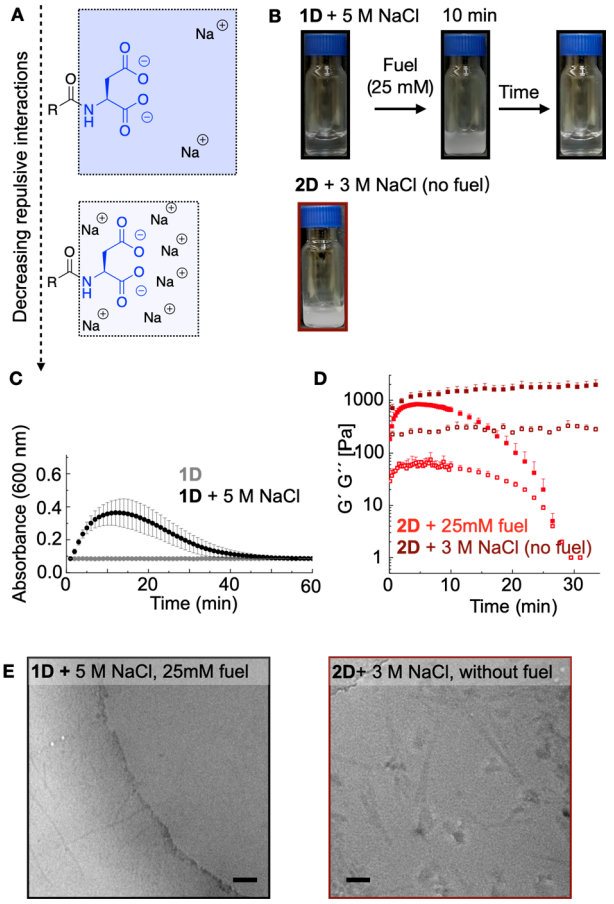


**Figure 3.** Regulating the response to fuel by tuning repulsive interactions. (A) Schematic representation of screening the repulsive interactions by the addition of salt. (B) Photographs of solutions of peptide **1D** (15 mM) with 5 M NaCl before and after the addition of 25 mM of fuel and **2D** (15 mM) with 3 M NaCl. (C) Turbidity measurements of 15 mM **1D** with or without salt in response to 25 mM of fuel against time. (D) Storage and loss modulus as a function of time, measured by plate−plate rheology of 15 mM **2D** with 3 M NaCl or with 25 mM EDC. Solid squares represent the storage modulus (G′); empty squares represent the loss modulus (G″). (E) Cryo-TEM images of the solutions of 15 mM **1D** + 5 M NaCl at 10 min after fueling with 25 mM EDC, and 15 mM **2D** with 3 M NaCl but without fuel. The error bars represent the standard deviation of the average ($n$ = 3). All scale bars correspond to 100 nm. All the experiments were carried out at a pH of 6 and in 200 mM MES buffer.

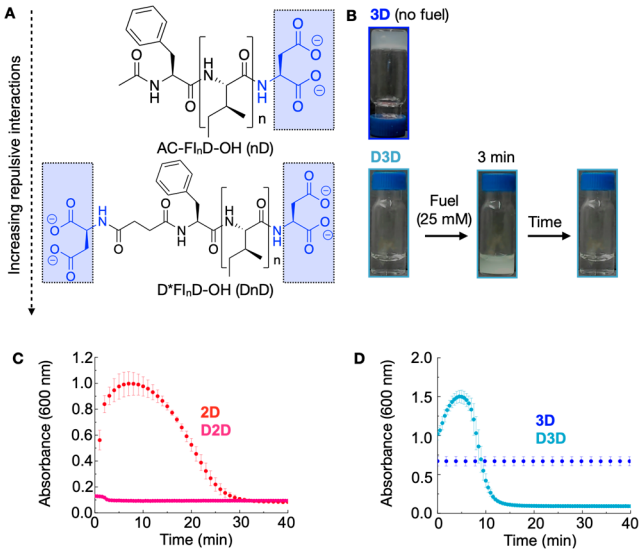


**Figure 4.** Regulating the response to fuel by tuning repulsive interactions in the molecular design. (A) Schematic representation of increasing the repulsive interactions by addition of charges. (B) Photographs of solutions of peptide **3D** (15 mM) without fuel addition and **D3D** (15 mM) before and after 25 mM fuel addition. (C) Turbidity measurements of **D2D** (15 mM) and **2D** (15 mM) in response to 25 mM fuel against time. (D) Turbidity measurements of **D3D** (15 mM) in response to 25 mM fuel against time compared with peptide **3D** (15 mM) without fuel. Error bars represent the standard deviation of the average ($n$ = 3). All the experiments were carried out at a pH of 6 and in 200 mM MES buffer.

could be permanently trapped in a self-assembled state by the addition of salt or acid.

From the data above, we can conclude that the response of the peptide can be regulated by controlling the electrostatic repulsion between precursor molecules. However, one could argue that the addition of 5 M of salt is not a particularly elegant design strategy. We thus designed a new peptide class where the increased electrostatic repulsion was encoded in the molecular structure (Figure 4A). We retained the C-terminal aspartate and added an additional aspartate to the N-terminus via a succinic acid spacer, resulting in D*FIID-OH (**D2D**) and D*FIIID-OH (**D3D**), where D* represents an aspartic acid amidated succinic acid spacer (Figure 4a). Consequently, the attractive interactions of **2D** remain roughly equal compared to **D2D**, but the number of carboxylate groups doubles, which results in an increase in repulsive interactions. We tested the response of these peptides to 25 mM EDC and compared it to the peptides without the additional repulsive interactions, i.e., D*FIID-OH (**D2D**) versus Ac-FIID-OH (**2D**) and D*FIIID-OH (**D3D**) versus Ac-FIIID-OH (**3D**). With that, we aim to study whether electrostatic repulsion, now encoded in the peptide design, can be used to regulate the response to chemical fuels.

We described earlier that peptide **3D** assembled into a hydrogel without any addition of fuel. In contrast, **D3D** did not assemble before the addition of fuel, which was proven by a ThT assay measurement (Figure S13). After the addition of fuel (25 mM EDC), the turbidity transiently increased (Figure 4B,C). The fuel-driven self-assembly of **D3D** was further confirmed by the transient formation of beta-sheets (Figure S14E). Importantly, both the turbidity and increased ThT signal fell back to their original level within 15 min. Considering the two aspartic acid groups **D3D**, we doubled the fuel to 50 mM compared to the experiments carried out with **3D**. Also, under these conditions, **D3D** underwent fuel-driven transient self-assembly (Figure S14A, C, E). These combined experiments showed that by increasing electrostatic repulsion in the molecular structure, we could change the peptide's behavior from a state where the precursors assembled to fuel-driven dissipative self-assembly.

We described earlier that **2D** self-assembled transiently in response to 25 mM of EDC as fuel. In contrast, peptide **D2D** showed a small and short increase in turbidity after the addition of fuel (25 or 50 mM EDC (Figure 4D and Figure S14D)). Meanwhile, a ThT assay demonstrated that peptide **D2D** did not engage significantly in beta-sheet formation in response to EDC (Figure S14F). These experiments show that by increasing the electrostatic interactions between the peptides by the incorporation of an extra aspartic acid, the


https://dx.doi.org/10.1021/jacs.0c04203
J. Am. Chem. Soc. 2020, 142, 14142−14149

behavior can be tuned from dissipative self-assembly to virtually no-assembly in response to fuel. Moreover, from the combined data set, we can conclude that the response of the peptide can be regulated by increasing electrostatic repulsion between peptides.

The combined experiments allow creating a phase diagram of the fuel-driven response of our peptides. In Figure 5A, on the *y*-axis, we show the number of isoleucines in the peptide design ($n$), as a measure for attractive interactions, against the concentration of added salt, like an inverted measure for the repulsive interactions. With increasing attractive interactions and no added salt, the system behavior evolves from no assembly, through dissipative self-assembly, to a state where the precursor assembles. Similarly, the addition of salt decreases the electrostatic repulsion and thus evolves the system from no assembly to dissipative assembly to a state where the precursor assembles. In Figure 5B, on the *y*-axis, again, we show the number of isoleucines in the peptide design ($n$). On the *x*-axis, we show the number of aspartic acid groups; 1 or 2 corresponds, for example, to **2D** or **D2D**, respectively. The *x*-axis is thus a measure for repulsive interactions. We found that on increasing that number, the behavior could be changed from dissipative assembly to no assembly or from a state where the precursor assembles to dissipative assembly.

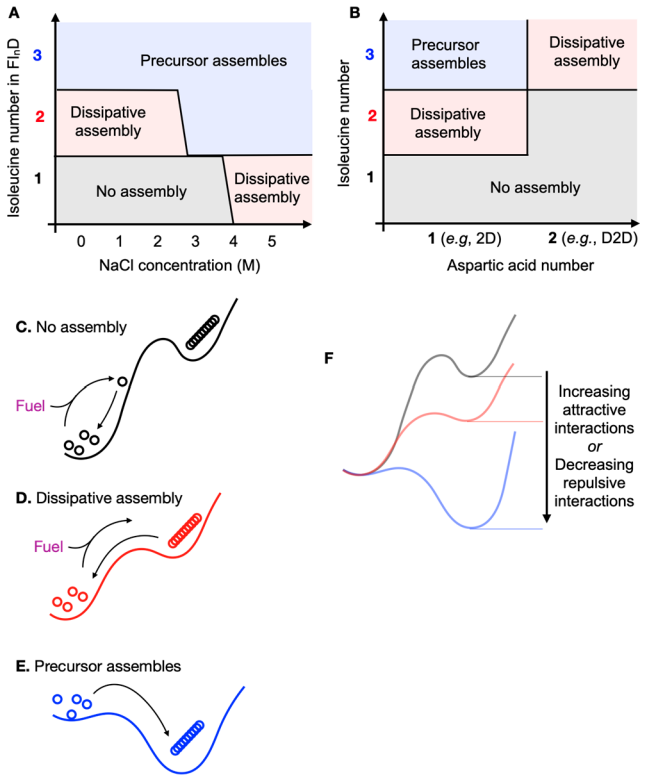


**Figure 5.** Phase diagrams and energy landscapes of chemically fueled assembly. (A) Possible peptide behavior with one, two, or three isoleucine residues in the peptide sequence Ac-FI$_n$D-OH at different salt concentrations. (B) Possible peptide behavior with one, two, or three isoleucine residues and one or two charged residues in the peptide sequence. (C−E) Energy landscapes of the three scenarios: no assembly, dissipative assembly, and the precursor assembles. (F) Combined energy landscape of the cases discussed in B−D.

The observed phase diagrams can be rationalized by the simplified energy landscapes of self-assembly (Figure 5C−E). These energy landscapes are characterized by at least two energy wells. One well represents the nonassembled precursor, and one represents the coassembled precursor and product state. The activation of the precursors pushes them up in the energy landscape, potentially in the next energy well, where self-assembly is favored. In the case of no assembly (Figure 5C), the energy gain upon activation is insufficient to drive the precursor into the next well, either because the attractive interactions are insufficient or the repulsive interactions are too great. In the case of dissipative assembly (Figure 5D), the energy gain upon activation can drive the precursor into the next well, where self-assembly takes place. Moreover, the energy barrier for disassembly is low; that is, disassembly takes place after deactivation without great delay. Finally, in the case where the precursor assembles, the energy well for assembly of the precursor is below the energy well for its nonassembled state (Figure 5E). The system thus favors the assembly of the precursor without the need for fuel.

In Figure 5F, we compare the three energy landscapes. In each of our experiments, the activation and deactivation are driven by the same chemical reaction cycle, and the energy gained upon activation is thus roughly similar. The difference in the behavior thus comes from the difference in the energy well of the self-assembled state relative to the energy well of the nonassembled state, which can be tuned by peptide designs. For example, when the number of attractive interactions is increased, the energy well corresponding to the self-assembled state is pushed downward relative to the nonassembled state. Similarly, when salt is added to the system, effectively decreasing the ionic repulsion between precursors, the energy well associated with the self-assembled state of the precursor and product is pushed down. We believe that these phase diagrams and their associated energy landscapes can be generalized to some degree for fuel-driven assemblies, provided that the design is based on a reaction cycle that uses charge abolishment as a mechanism to induce self-assembly.

## CONCLUSION

We introduced a new family of peptides coupled to a well-known chemically fueled reaction cycle. The simplicity of the peptide design and reaction cycle allows creating some general rules for the self-assembly behavior in response to fuel. We find three possible behaviors: the peptide does not assemble, it assembles dissipatively, or it assembles without fuel. We can toggle between these behaviors with different peptide designs and environmental conditions. Future work should investigate further nuances in these energy landscapes to probe other dynamic behaviors such as kinetic trapping or dynamic instabilities.

## ASSOCIATED CONTENT

### Supporting Information

The Supporting Information is available free of charge at https://pubs.acs.org/doi/10.1021/jacs.0c04203.

Materials and methods description and additional turbidity data, fluorescence spectroscopy data, rheology data, NMR data, and *cryo*-TEM images (PDF)



https://dx.doi.org/10.1021/jacs.0c04203
J. Am. Chem. Soc. 2020, 142, 14142−14149

## AUTHOR INFORMATION


### Corresponding Author

**Job Boekhoven** − *Department of Chemistry and Institute for Advanced Study, Technical University of Munich, 85748 Garching, Germany;* orcid.org/0000-0002-9126-2430; Email: job.boekhoven@tum.de

### Authors

**Kun Dai** − *Department of Chemistry, Technical University of Munich, 85748 Garching, Germany*

**Jennifer Rodon Fores** − *Department of Chemistry, Technical University of Munich, 85748 Garching, Germany;* orcid.org/0000-0002-7472-1228

**Caren Wanzke** − *Department of Chemistry, Technical University of Munich, 85748 Garching, Germany*

**Benjamin Winkeljann** − *Department of Mechanical Engineering and Munich School of Bioengineering, Technical University of Munich, 85748 Garching, Germany;* orcid.org/0000-0002-6334-6696

**Alexander M. Bergmann** − *Department of Chemistry, Technical University of Munich, 85748 Garching, Germany*

**Oliver Lieleg** − *Department of Mechanical Engineering and Munich School of Bioengineering, Technical University of Munich, 85748 Garching, Germany;* orcid.org/0000-0002-6874-7456

Complete contact information is available at: https://pubs.acs.org/10.1021/jacs.0c04203


### Notes

The authors declare no competing financial interest.

## ACKNOWLEDGMENTS

K.D. thanks the financial support from the China Scholarship Council. J.R.F. thanks the Deutsche Forschungsgemeinschaft for project 411722921. J.B., W.B., and O.L. acknowledge funding from the Deutsche Forschungsgemeinschaft (DFG, German Research Foundation), SFB- 863, Project ID 111166240 (Project B11). C.W. is grateful for funding by the Deutsche Forschungsgemeinschaft (DFG, German Research Foundation), Project-ID 364653263, TRR 235. J.B. is grateful for funding by the Technical University of Munich, Institute for Advanced Study, funded by the German Excellence Initiative and the European Union Seventh Framework Program under grant agreement No. 291763.

## REFERENCES


(1) van Rossum, S. A. P.; Tena-Solsona, M.; van Esch, J. H.; Eelkema, R.; Boekhoven, J. Dissipative Out-of-Equilibrium Assembly of Man-Made Supramolecular Materials. *Chem. Soc. Rev.* **2017**, *46* (18), 5519−5535.

(2) De, S.; Klajn, R. Dissipative Self-Assembly Driven by the Consumption of Chemical Fuels. *Adv. Mater.* **2018**, *30* (41), 1706750.

(3) Sorrenti, A.; Leira-Iglesias, J.; Markvoort, A. J.; de Greef, T. F. A.; Hermans, T. M. Non-Equilibrium Supramolecular Polymerization. *Chem. Soc. Rev.* **2017**, *46* (18), 5476−5490.

(4) Merindol, R.; Walther, A. Materials Learning from Life: Concepts for Active, Adaptive and Autonomous Molecular Systems. *Chem. Soc. Rev.* **2017**, *46* (18), 5588−5619.

(5) Rieß, B.; Grötsch, R. K.; Boekhoven, J. The Design of Dissipative Molecular Assemblies Driven by Chemical Reaction Cycles. *Chem.* **2020**, *6* (3), 527.

(6) Molla, M. R.; Rangadurai, P.; Antony, L.; Swaminathan, S.; de Pablo, J. J.; Thayumanavan, S. Dynamic Actuation of Glassy Polymersomes through Isomerization of a Single Azobenzene Unit at the Block Copolymer Interface. *Nat. Chem.* **2018**, *10* (6), 659−666.

(7) Brouhard, G. J.; Rice, L. M. Microtubule Dynamics: An Interplay of Biochemistry and Mechanics. *Nat. Rev. Mol. Cell Biol.* **2018**, *19* (7), 451−463.

(8) Dogterom, M.; Koenderink, G. H. Actin−Microtubule Crosstalk in Cell Biology. *Nat. Rev. Mol. Cell Biol.* **2019**, *20* (1), 38−54.

(9) Wang, G.; Liu, S. Strategies to Construct a Chemical-Fuel-Driven Self-Assembly. *ChemSystemsChem.* **2020**, DOI: 10.1002/syst.201900046.

(10) Kim, B. J.; Yang, D.; Xu, B. Emerging Applications of Supramolecular Peptide Assemblies. *Trends in Chemistry* **2020**, *2* (1), 71−83.

(11) Ragazzon, G.; Prins, L. J. Energy Consumption in Chemical Fuel-Driven Self-Assembly. *Nat. Nanotechnol.* **2018**, *13* (10), 882−889.

(12) Pappas, C. G.; Sasselli, I. R.; Ulijn, R. V. Biocatalytic Pathway Selection in Transient Tripeptide Nanostructures. *Angew. Chem., Int. Ed.* **2015**, *54* (28), 8119−8123.

(13) Boekhoven, J.; Brizard, A. M.; Kowlgi, K. N. K.; Koper, G. J. M.; Eelkema, R.; van Esch, J. H. Dissipative Self-Assembly of a Molecular Gelator by Using a Chemical Fuel. *Angew. Chem., Int. Ed.* **2010**, *49* (28), 4825−4828.

(14) Leira-Iglesias, J.; Sorrenti, A.; Sato, A.; Dunne, P. A.; Hermans, T. M. Supramolecular Pathway Selection of Perylenediimides Mediated by Chemical Fuels. *Chem. Commun.* **2016**, *52* (58), 9009−9012.

(15) Leira-Iglesias, J.; Tassoni, A.; Adachi, T.; Stich, M.; Hermans, T. M. Oscillations, Travelling Fronts and Patterns in a Supramolecular System. *Nat. Nanotechnol.* **2018**, *13* (11), 1021−1027.

(16) Sorrenti, A.; Leira-Iglesias, J.; Sato, A.; Hermans, T. M. Non-Equilibrium Steady States in Supramolecular Polymerization. *Nat. Commun.* **2017**, *8*, 15899.

(17) Tena-Solsona, M.; Janssen, J.; Wanzke, C.; Schnitter, F.; Park, H.; Rieß, B.; Gibbs, J. M.; Weber, C. A.; Boekhoven, J. *ChemRxiv* **2019**, Preprint DOI: 10.26434/Chemrxiv.9978539.V1.

(18) Tena-Solsona, M.; Wanzke, C.; Riess, B.; Bausch, A. R.; Boekhoven, J. Self-Selection of Dissipative Assemblies Driven by Primitive Chemical Reaction Networks. *Nat. Commun.* **2018**, *9* (1), 2044.

(19) Debnath, S.; Roy, S.; Ulijn, R. V. Peptide Nanofibers with Dynamic Instability through Nonequilibrium Biocatalytic Assembly. *J. Am. Chem. Soc.* **2013**, *135* (45), 16789−16792.

(20) Maiti, S.; Fortunati, I.; Ferrante, C.; Scrimin, P.; Prins, L. J. Dissipative Self-Assembly of Vesicular Nanoreactors. *Nat. Chem.* **2016**, *8* (7), 725−731.

(21) Heinen, L.; Walther, A. Programmable Dynamic Steady States in ATP-Driven Nonequilibrium DNA Systems. *Science Advances* **2019**, *5* (7), No. eaaw0590.

(22) Heuser, T.; Weyandt, E.; Walther, A. Biocatalytic Feedback-Driven Temporal Programming of Self-Regulating Peptide Hydrogels. *Angew. Chem., Int. Ed.* **2015**, *54* (45), 13258−13262.

(23) Panja, S.; Dietrich, B.; Adams, D. J. Chemically Fuelled Self-Regulating Gel-to-Gel Transition. *ChemSystemsChem.* **2020**, *2* (1), DOI: 10.1002/syst.201900038.

(24) Ragazzon, G.; Baroncini, M.; Silvi, S.; Venturi, M.; Credi, A. Light-Powered Autonomous and Directional Molecular Motion of a Dissipative Self-Assembling System. *Nat. Nanotechnol.* **2015**, *10* (1), 70−75.

(25) Grötsch, R. K.; Wanzke, C.; Speckbacher, M.; Angı, A.; Rieger, B.; Boekhoven, J. Pathway Dependence in the Fuel-Driven Dissipative Self-Assembly of Nanoparticles. *J. Am. Chem. Soc.* **2019**, *141* (25), 9872−9878.

(26) Grötsch, R. K.; Angı, A.; Mideksa, Y. G.; Wanzke, C.; Tena-Solsona, M.; Feige, M. J.; Rieger, B.; Boekhoven, J. Dissipative Self-Assembly of Photoluminescent Silicon Nanocrystals. *Angew. Chem., Int. Ed.* **2018**, *57* (44), 14608−14612.

(27) Wang, G.; Tang, B.; Liu, Y.; Gao, Q.; Wang, Z.; Zhang, X. The Fabrication of a Supra-Amphiphile for Dissipative Self-Assembly. *Chem. Sci.* **2016**, *7* (2), 1151−1155.
(28) Boekhoven, J.; Hendriksen, W. E.; Koper, G. J. M.; Eelkema, R.; van Esch, J. H. Transient Assembly of Active Materials Fueled by a Chemical Reaction. *Science* **2015**, *349* (6252), 1075−1079.
(29) Tena-Solsona, M.; Rieß, B.; Grötsch, R. K.; Löhrer, F. C.; Wanzke, C.; Käsdorf, B.; Bausch, A. R.; Müller-Buschbaum, P.; Lieleg, O.; Boekhoven, J. Non-Equilibrium Dissipative Supramolecular Materials with a Tunable Lifetime. *Nat. Commun.* **2017**, *8*, 15895.
(30) Wanzke, C.; Jussupow, A.; Kohler, F.; Dietz, H.; Kaila, V. R. I.; Boekhoven, J. Dynamic Vesicles Formed By Dissipative Self-Assembly. *ChemSystemsChem.* **2020**, DOI: 10.1002/syst.201900044.
(31) Rieß, B.; Wanzke, C.; Tena-Solsona, M.; Grötsch, R. K.; Maity, C.; Boekhoven, J. Dissipative Assemblies That Inhibit Their Deactivation. *Soft Matter* **2018**, *14* (23), 4852−4859.
(32) Kariyawasam, L. S.; Hartley, C. S. Dissipative Assembly of Aqueous Carboxylic Acid Anhydrides Fueled by Carbodiimides. *J. Am. Chem. Soc.* **2017**, *139* (34), 11949−11955.
(33) Sahoo, J. K.; Nazareth, C.; VandenBerg, M. A.; Webber, M. J. Aromatic Identity, Electronic Substitution, and Sequence in Amphiphilic Tripeptide Self-Assembly. *Soft Matter* **2018**, *14* (45), 9168−9174.
(34) Evans, D. F.; Wennerström, H. *The Colloidal Domain: Where Physics, Chemistry, Biology, and Technology Meet*, 2nd ed.; Advances in Interfacial Engineering Series; Wiley-VCH: New York, 1999.


https://dx.doi.org/10.1021/jacs.0c04203
*J. Am. Chem. Soc.* 2020, 142, 14142−14149